European Geothermal Congress 2016
Strasbourg, France, 19-24 Sept 2016

Modelling seismic event location errors at the reservoir scale: application to the geothermal site of Soultz-sous-Forêts (Alsace, France)

X. Kinnaert[1,2*], E. Gaucher[1], T. Kohl[1] and U. Achauer[2]

[1] Karlsruhe Institute of Technology, Institute of Applied Geosciences, Geothermal Research, Karlsruhe, Germany

[2] EOST-IPGS UMR7516, Strasbourg, France

xavier.kinnaert@kit.edu

Keywords: location inaccuracy, location uncertainty, seismic monitoring, network design, EGS

ABSTRACT

The location of natural or induced earthquakes is of primary interest for geothermal fields monitoring and characterization. We investigate the impact of several parameters on earthquake absolute location errors. A two-steps approach is applied. First, body-waves travel-times between synthetic earthquake locations and seismic receiver positions are calculated. Then, the obtained travel-times are used as observed arrival-times. However, several of the initial hypotheses are changed before relocation to represent the lack of knowledge or simplifications which are investigated.

The method is applied to the geothermal site of Soultz-sous-Forêts (France). In 2000, a massive water injection was performed at approximately 5 km depth, in the granitic basement, to enhance the GPK2 well productivity. A downhole and a surface network recorded several thousands of induced micro-earthquakes. In this work, we quantify the location variation due to the joint use of the downhole and surface networks, or to the use of one of those networks. Besides the description of the usual location uncertainties, the impact of the picking time precision is investigated as well as the variation of the velocity model to mimic the possible effect of a massive water injection.

The downhole network is proven to be useful to decrease the location uncertainty obtained from the surface network alone. Nevertheless, the locations computed using this network may be more biased.

1. INTRODUCTION

In geothermal applications, the location of natural or induced earthquakes is of primary interest. This parameter will be used for seismic risk mitigation but also to characterize the active faults and fractures of the geothermal reservoir. Earthquake hypocentres are often seen as single points in a 3D space however location errors exist and determine the scale at which results can be interpreted. For geothermal reservoir studies, location errors sometimes lower than 100 m may lead to misinterpretation of the sub-surface (Kinnaert *et al.* 2016). Hence, quantifying the error associated with an earthquake location is of primary importance to carry reliable result analysis.

The earthquake location error can be described as the combination of the location inaccuracy and the location uncertainty. The location uncertainties are directly linked to the uncertainties which are taken into account during the location process (Tarantola 2005), typically *a priori* picking uncertainties of seismic wave arrivals, and contribute to *a posteriori* location uncertainties. On the contrary, the location inaccuracy is defined as the wrong positioning of the earthquake hypocentre due to all effects that have been ignored in the inverse problem. These simplifications of the reality introduce systematic errors, or bias, in the computation of the earthquake location. Usually, a velocity model not representative of the effective seismic propagation medium leads to earthquake location inaccuracies (Pavlis 1986; Husen, Kissling and Deschwanden 2013). Location inaccuracy quantification requires the application of specific procedures and consequently they are not often studied.

This work focuses on location inaccuracies and uncertainties of absolute earthquake location. The method developed is applied on the geothermal site of Soultz-sous-Forêt (France) on which many studies have been done. In this paper, the main investigation concerns the impact of the seismic network design on the location errors. The method to quantify location inaccuracies and uncertainties is first described. Then, the Soultz geothermal site is presented. The impact of the different seismic network coverages is quantified and the possible effect on sub-surface interpretation is discussed. The effect of picking time precision is also

investigated. At last the velocity model is perturbed to mimic the impact of massive water injection.

2. METHODOLGY

To quantify the seismic event location uncertainties and inaccuracies, a two-steps method is applied. During the synthetic modelling step, travel-times of body waves are calculated between synthetic sources and the position of different seismic sensors. In this step, the assumptions are supposed to represent the reality of the sub-surface. The travel-times are computed using the finite-difference method of Podvin and Lecomte (1991) implemented in the NonLinLoc software (Lomax 2011). In the second step, the travel-times obtained in the synthetic modelling step are considered as observations and are used to (re-)locate the synthetic seismic event. Nevertheless, few modifications are introduced in the input data (velocity model, seismic network, time uncertainty and precision). The location is performed using the NonLinLoc software (Lomax, Michelini and Curtis 2009) and the grid-search method which provides a complete probability density function (PDF) of the event hypocentre in any 3D velocity model. This software has the advantage to keep the non-linearity of the location inverse problem, to apply the Bayesian formalism proposed by Tarantola and Valette (1982) and to use the methodology of Wittlinger, Herquel and Nakache (1993). For simplicity, we define the location uncertainty as the half-length of the longest axis of the PDF for the 68.3% confidence level, assuming a Gaussian posterior distribution (Lomax 2011). The inaccuracy is calculated by comparing the hypocentre position obtained after location with the initial synthetic hypocentre and corresponds to the Cartesian distance.

3. THE SOULTZ GEOTHERMAL SITE

3.1. Geological settings

The Soultz-sous-Forêts geothermal site is located in the Upper Rhine Graben (URG), in France. The geological and structural settings of the shallow sub-surface in the URG are well known due to earlier investigations from the oil industry (Schnaebele 1948). At Soultz, seismic profiles provided good knowledge of the sedimentary cover in the Soultz area and highlighted numerous horst and grabens (Wentzel and Brun 1991).

Because of the presence of fracture networks in the sub-surface and thermal anomalies (Bailleux *et al.* 2013), the URG is suitable for geothermal energy development. Besides Soultz, several deep geothermal sites exist (Landau, Insheim, Bruchsal) or are under development (Rittershoffen, Gross-Gerau).

At Soultz, two main reservoirs have been developed at around 3500 m and 5000 m depth in the granitic basement. The temperature reaches about 200°C in the deepest one (Baumgärtner *et al.* 2000). The highly fractured Paleozoic granitic basement is overlaid by about 1400 m of sediments from tertiary and quaternary eras (Genter *et al.* 2010).

3.2. Seismicity induced in 2000

In 2000, the well GPK2 was stimulated by a massive water injection which induced several thousands of micro-earthquakes (Cuenot, Dorbath and Dorbath 2008) recorded by downhole and surface seismic stations. Cuenot et al (2008) were the first to combine the data from both networks to locate the induced seismicity. 7215 events were located in the granite, between 4000 and 5500 m depth. The seismic cloud is oriented N30°W and, referencing to GPK1 wellhead, extends about -2.5 km to the North and about -1.5 km to the East with a rotation of about 30° counter-clockwise. In the present paper, as in many other studies, the earthquake catalogue resulting from the work of Cuenot *et al.* (2008) is used as a reference database.

3.3. Reference velocity model

The seismic velocity model used by Cuenot (2009) is taken as a reference. Velocities always increase with depth. In our work, this model is always used to relocate the synthetic sources. The P-wave velocity ranges from 1800 m/s at surface to 5800 m/s at the top of the non-altered granitic layer, which is located at ~1700 m depth. The largest velocity contrast is observed at the sediment-altered granite interface, close to 1400 m depth. The S-wave velocity ranges from 860 m/s at surface to 3300 m/s in the non-altered granitic basement. The Vp/Vs ratio is not constant over depth and varies between 1.75 in the granite and 2.15 in the shallowest sedimentary layer. The seismicity induced in 2000 in the deepest reservoir is located in the non-altered granite.

3.4. Seismic monitoring networks

In 2000, the seismic monitoring of the GPK2 stimulation was carried out using a downhole network and a surface network (Cuenot *et al.;* Cuenot *et al.* 2008) (Figure 1). Three accelerometers (in wells 4550, 4601 and OPS4 at ~1500 m depth) and two hydrophones (in wells EPS1 and GPK1 at ~2000 m and ~3500 m depth respectively) constitute the downhole network (Dyer 2001). The surface seismic network was composed of eight vertical component sensors and nine 3C-sensors. To be consistent with the work of Cuenot *et al.* (2008) and the associated reference catalogues of the pickings and location of the induced seismicity, the EPS1 sensor is not used in this study to mimic the lack of reliable picking at this station. Similarly, three 3C-sensors of the surface network (belonging to the ReNaSS) were not used.

According to the Soultz seismic monitoring, three network designs may be used to locate the earthquake

hypocentres: i) the downhole network of the four usable borehole sensors (red triangles in Figure 1), ii) the surface network with 14 usable sensors (green triangles), and iii) the combination of both previous networks called the "combined network" in the following. Each of those three networks is used separately in all cases investigated in the following.

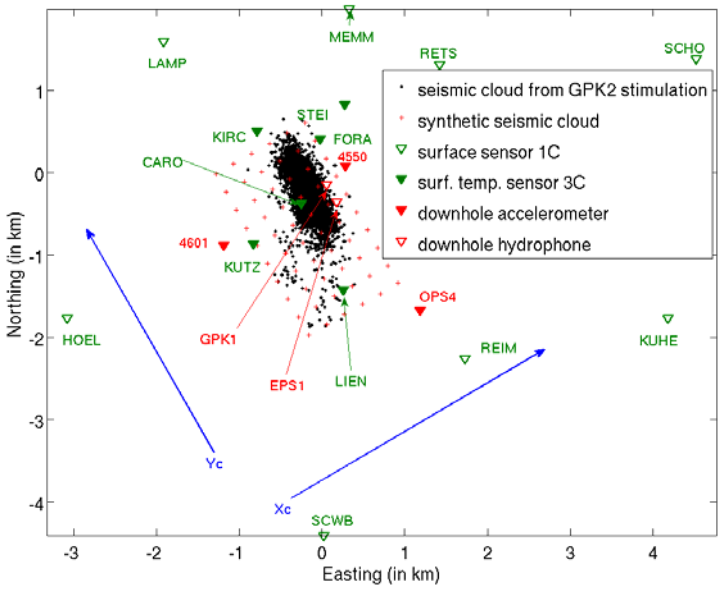

Figure 1: Geometry of the seismic networks monitoring during the stimulation of the well GPK2 in June-July 2000. The filled triangles stand for 3C-sensors whereas the empty symbols stand for mono-component geophones. Red and green triangles show the position of the downhole and surface sensors respectively. The projections of the synthetic (crosses) and real (dots) seismic clouds (Cuenot 2009) are also represented. The blue arrows show the Xc and Yc axes used in this study which correspond to a rotation of N30°W around the vertical axes of the East and North axes. Easting and Northing are given relative to GPK1 well-head.

3.5. Synthetic event hypocentres

To investigate the location errors, we create a synthetic seismic cloud (red crosses in Figure 1), which is representative of that obtained for the stimulation of GPK2 (black dots), and define it in a system rotated by 30° anti-clockwise around the vertical axis. In this system described by the Xc, Yc and vertical axes (Figure 1) and used as reference from now on, the synthetic sources are distributed every 125 m in each direction. They extend from -4 to -5.5 km in depth (all depths given in this paper are true vertical depth from mean sea level, TVD MSL, unless specified differently), from -1.125 to 0.125 km along Xc, and from -1.625 to 0.625 km along Yc. All coordinates are given with respect to the GPK1 well-head. Most of the real seismic events belong to the NE quarter of the synthetic event zone. Besides this 3D-synthetic cloud of events, a set of three planes may be used. The extension of the planes is similar to the extension of the 3D grid and they all cut the well at the mid-point of the GPK2 open-hole section. Hence, a horizontal plane is located at a depth of 4529 m, a vertical plane oriented along Xc is located 311 m south of GPK1 and one oriented along Yc is located 234 m west.

4. RESULTS AND DISCUSSION

4.1. Location uncertainties

To quantify the location uncertainties, picking uncertainty of ±5 ms and ±15 ms were applied to the modelled seismic travel-times at the downhole and the surface stations respectively. The P- and S-waves uncertainties were taken similar. These values are consistent with the reference picking catalogue of Cuenot *et al.* (2008). In the modelling and location steps, the reference 1D velocity model is used and discretized on a 12.5 m mesh. All sources of the 3D grid are used. Both the synthetic modelling and the location were computed in the reference velocity model.

Figure 2 shows statistics of the earthquake location uncertainties along the depth directions using boxplots (Tukey 1977). The boxplots display the median, the first (25%, Q1) and third (75%, Q3) quartiles, and the range of the considered variable. The location uncertainty obtained from the combined network increases almost linearly with increasing depth. The median reaches about 73 m at 5500 m and the maximum of 77 m in the deepest part. Such an evolution is not seen along the Xc and Yc axes. The

location uncertainty increases to the North and to the South along Xc from a point of latitude close to the mid-point of GPK2 open-hole section. In the NE part of the synthetic cloud, the absolute locations can have uncertainties with a median ~65 m and a maximum Q3 ~70 m depending on the source depth. The obtained uncertainties are a bit smaller than the 80-100 m mean uncertainties given by Cuenot *et al.* (2008).

Locating using the downhole network alone leads to location uncertainties of the order of 65-95 m as a median value and a maximum uncertainty of about 105 m. Because of the relative proximity of the sensors to the synthetic seismic cloud and the relatively small picking uncertainties (±5 ms), the obtained hypocentres are more precise (Figure 2). On the contrary, locations calculated with the surface network alone lead to larger uncertainties. In the worst case, uncertainty of ~150 m is obtained.

This test shows that the downhole network has a strong influence on the location uncertainties. Furthermore, the downhole network better constrains the location uncertainties in the South direction along Yc while the surface network better constrains the location uncertainties in the North along Yc. Finally, one can see that the downhole network provides better depth control of the event hypocentres, especially for the shallower earthquakes.

These amplitude and spatial distributions of the uncertainties will remain very similar in the following tests performed in this paper.

4.2. Location errors due to inaccuracies in the input arrival-times

Many software used for processing earthquake location as well as picking seismograms work with input arrival-time picking accuracy rounded at 10 ms. Such a picking accuracy is given in the reference picking catalogue of the 2000 induced seismicity. Here, we quantify the possible effects induced by this picking inaccuracy at Soultz. To do so, we rounded to the nearest 10 ms the travel-times of the modelling step prior to location. All sources of the 3D grid are used. Both the synthetic modelling and the location were computed in the reference velocity model.

No significant vertical inaccuracy has been obtained in any direction and for all tested networks the absolute values of Q1 and Q3 are always smaller than or equal to the mesh size used for the location process. For the combined network, observed (total) inaccuracies are of the order of 15 to 30 m as median values with the smallest inaccuracies in the eastern and southern part of the 3D-synthetic sources and for the shallowest events. A maximum bias of ~60 m is obtained.

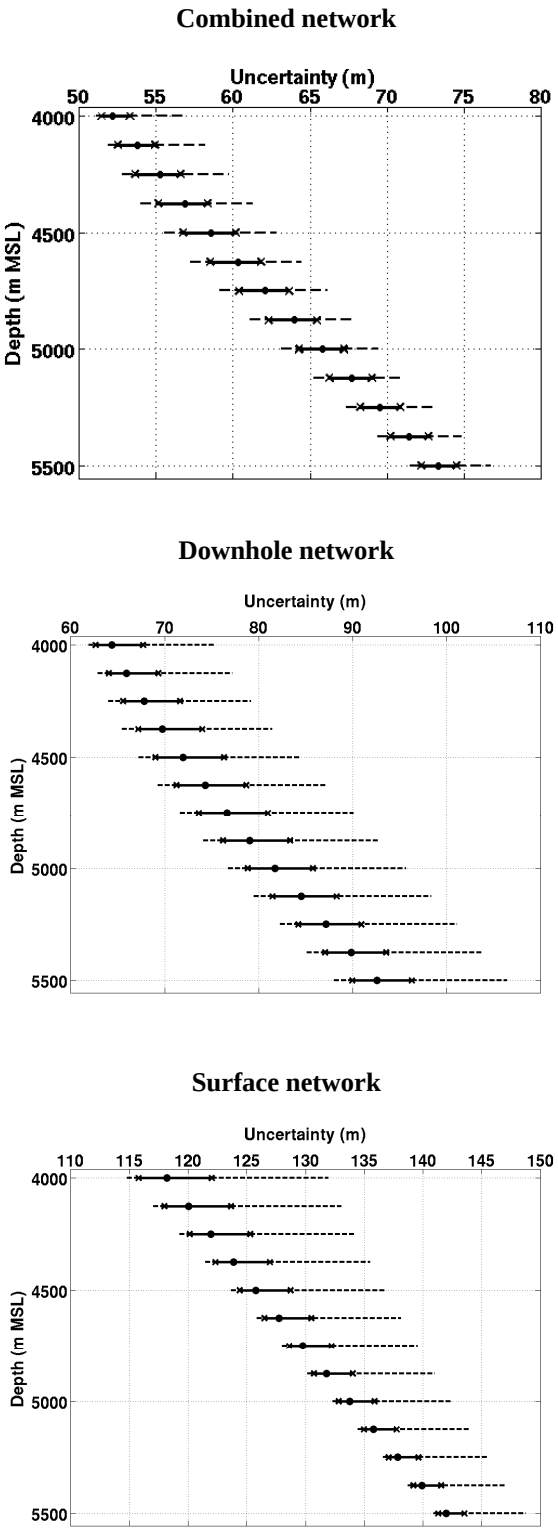

Figure 2: Boxplots of the location uncertainties along depth of the 3D-synthetic earthquakes. Results from the combined (top), downhole (middle) and surface (bottom) networks. The boxplots show the range of values (dashed lines), the first and third quartile (crosses) and the median (disk).

The downhole network alone leads in general to global locations inaccuracies with median between 30 and 40 m and with variations similar for the horizontal inaccuracy alone. A bias up to ~95 m can be found for the less accurate locations at depth and in the northern part of the synthetic cloud. This means that performing event location using the downhole network alone leads to inaccuracies ~1.5 larger than those obtained with the combined network.

Bias modelled for locations performed with the surface network alone are lower than the one obtained for the combined network. Global inaccuracies smaller than 20 m are found as a median case in all direction of the cubic cloud whereas the Q3 value does not exceed 30 m and a maximum bias of about 50 m is seen for the deepest sources almost in the middle of the 3D-synthetic cloud.

As an explanation, let us consider the position of the different sensor relative to the source initial locations. The downhole sensors are the nearest to the synthetic earthquakes. Therefore, the travel-times for any phase to arrive at the station are shorter than for the surface sensors. Consequently, rounding at 10 ms has a larger impact on the travel-times for the downhole network than for the surface network. Hence, adding the downhole sensors in the case of rounded picks adds stronger incorrect observations and consequently leads to larger bias.

4.3. Impact of the stimulation zone

The impact of a massive water injection is important for studies on induced seismicity due to well hydraulic stimulation or circulation tests. To model the effect of the fluid injection, we follow the synthetic test performed by Calò *et al.* (2011). At depths between 4030 and 5030m in a radius of 375 m around the mid-point of the open-hole section of the well GPK2, P- and S-wave velocities have been decreased by 10% and 5% respectively. In this part, the event locations are computed in the reference 1D velocity model but the travel-times were computed in the perturbed velocity model. The synthetic sources are distributed on the three orthogonal planes crossing GPK2 at the middle of the open-hole section.

No significant location inaccuracy is observed for any network for sources positioned shallower than the stimulated zone. Moreover, the location inaccuracies are mainly horizontal since the vertical inaccuracies are always smaller than one grid-cell. Nevertheless, the results obtained for the combined network show a significant decrease of location accuracy (Figure 3 top panels). It increases through the injection zone and reaches about 100 m as median value of horizontal bias at its bottom, for sources located on the vertical-Xc plane. A maximum horizontal bias of about 150 m can be observed for these sources. When the sources were initially positioned on the vertical-Yc plane, the median horizontal inaccuracy can reach 75 m in depth and the maximum is about 90 m. The events tend to be located away from their initial position in a direction opposite to the simulated stimulation zone. Interestingly, the origin times of the events are as accurate as for the ideal case.

For the locations computed with the surface network, the inaccuracies are of the same order as or smaller than the corresponding uncertainties.

For locations computed with the downhole network (Figure 3 middle panels), median inaccuracy of about 130 m, which is about 1.3 times the 95 m of the location uncertainty, can be observed in the deepest part of the Xc-vertical plane of sources. For the same source location, the combined network leads to ~110 m inaccuracy, about 1.4 times the uncertainty. Furthermore, if we look at the inaccuracy variation along the Xc axis, the median value reaches 80 m, which is 1.25 times the median value of the uncertainty, in the eastern part. The Q3 difference is even larger than the median difference (120 m for the Q3 inaccuracy and 75 m for the Q3 uncertainty). Taken the extreme values into account, the inaccuracies can be two times larger than the uncertainties for the combined network, leading to bias of about 150 m with uncertainties of about 75 m.

5. CONCLUSION AND OUTLOOKS

In this paper, we mainly focused on the impact of several seismic network configurations on earthquake location errors, discriminating uncertainty from inaccuracy. The methodology was applied to a synthetic data set representative of the seismicity induced during the stimulation of the GPK2 well at Soultz-sous-Forêts.

The combination of a surface and a downhole network provides the most certain hypocentre locations, of the order of 55 m to 75 m in the denser part of the seismic cloud. This result is compatible with the estimates from Cuenot *et al.* (2008). However, we show that the uncertainty is not homogeneously distributed in space and is larger in the NE than in the SW and increases with depth. Consequently, the implementation of the downhole network allows decreasing by a factor of two the location uncertainties compared to those which would be obtained from the surface network.

P- and S-wave arrival-times rounded at 10 ms, as written in the existing picking catalogue, leads mainly to horizontal location inaccuracy up to 20-30 m for locations computed with the combined network. The picking inaccuracy generates stronger bias for sources which are deep or in the NE part of the seismic cloud. Nevertheless, the location inaccuracies remain usually three times smaller than the location uncertainties and

may be considered as negligible. The rounding effect induces location inaccuracies 50% larger with the downhole network than with the surface network. Hence, the downhole network is useful to diminish the location uncertainty but leads to stronger location bias.

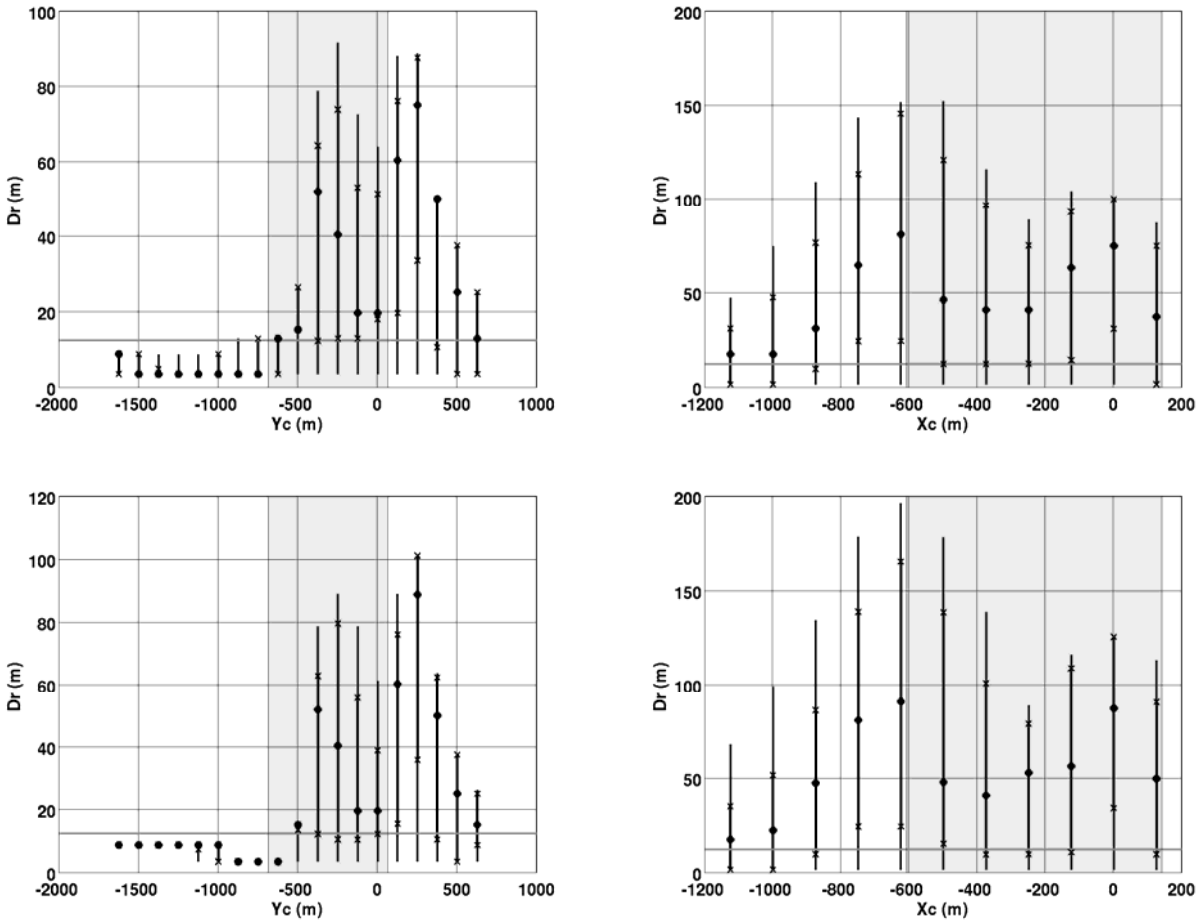

Figure 3: Boxplots of the location inaccuracies computed in the perturbed velocity model. Results of the combined network (top panels) and of the downhole network alone (bottom panels) are shown, for the sources on the vertical-Yc plane (left column) and on the vertical-Xc plane (right column). The thick grey line at 12.5 m represents the mesh size used for locating and the grey zone corresponds to the simulated injection zone. The boxplots symbols are described in Figure 2.

The impact of the water stimulation around GPK2 simulated by 10 % and 5 % decreases of the P- and S-wave velocity respectively was investigated. This does neither affect significantly the location uncertainties nor the vertical accuracies. Not taking into account the low velocity zone leads to significant location inaccuracies of the order of the location uncertainties but usually not larger. Unfortunately, bias larger than 100 m should be expected for events in the deep-eastern part using the combined network, because location inaccuracies are not homogeneous in space. This value is larger than the 75 m of uncertainty, which means that the real hypocentre is not included in the 68.3% confidence level. Interestingly, the impact of the velocity decreases can be observed for several hypocentres obtained by the combined network or by the downhole network but not computed by the surface network due to the associated larger location uncertainties.

These conclusions are associated with absolute location methods. Nevertheless, the improvement or worsening brought by relative location methods should be also investigated since the latter become routinely used to locate earthquakes. The proposed methodology could be used in similar reservoir monitoring contexts to characterize the capabilities of the existing or expected seismicity to describe the reservoir.

REFERENCES

Bailleux P., Schill E., Edel J.-B. and Mauri G. 2013. Localization of temperature anomalies in the Upper Rhine Graben: insights from geophysics and

neotectonic activity. *International Geology Review* **55**.

Baumgärtner J., Gérard A., Baria R. and Garnisch J. 2000. Progress at the European HDR project at Soultz-sous-Forêts: preliminary results from the deepening of the well GPK2 to 5000 m, SPE International Petroleum Conference and Exhibition, Villahermosa, Mexico.

Calò M., Dorbath C., Cornet F.H. and Cuenot N. 2011. Large-scale aseismic motion identified through 4-D P-wave tomography. *Geophysical Journal International* **186** (3), 1295–1314.

Cuenot N. 2009. *Réponse du granite fracturé de Soultz-sous-Forêts à des injections massives de fluide: Analyse de la microsismicité induite et du régime de contraintes*.

Cuenot N., Dorbath C. and Dorbath L. 2008. Analysis of the microseismicity induced by fluid injections at the EGS site of Soultz-sous-Forêts (Alsace, France): Implications for the characterization of the geothermal reservoir properties. *Pure and Applied Geophysics* **165** (5), 797–828.

Dyer B.C. 2001. *Soultz GPK2 stimulation June/July 2000*. Seismic monitoring report S.

Genter A., Evans K., Cuenot N., Fritsch D. and Sanjuan B. 2010. Contribution of the exploration of deep crystalline fractured reservoir of Soultz to the knowledge of enhanced geothermal systems (EGS). *Comptes Rendus Geoscience* **342** (7-8), 502–516.

Husen S., Kissling E. and Deschwanden A. 2013. Induced seismicity during the construction of the Gotthard Base Tunnel, Switzerland: hypocenter locations and source dimensions. *Journal of Seismology* **17** (1), 63–81.

Kinnaert X., Gaucher E., Achauer U. and Kohl T. 2016. Modelling earthquake location errors at a reservoir scale: a case study in the Upper Rhine Graben. *Geophysical Journal International* **accepted**.

Lomax A. 2011. *NonLinLoc: Probabilistic, Non-Linear, Global-Search Earthquake Location in 3D media*. ALomax Scientific.

Lomax A., Michelini A. and Curtis A. 2009. Earthquake location , Direct, Global-Searc Methods. In: *Encyclopedia of Complexity and Systems Science* (ed. R.A. Meyers), pp. 2449–2473. Springer New York. ISBN 978-0-387-75888-6.

Pavlis G.L. 1986. Appraising earthquake hypocenter location errors: A complete, practical approach for single-event locations. *Bulletin of the Seismological Society of America* **76** (6), 1699–1717.

Podvin P. and Lecomte I. 1991. Finite difference computation of traveltimes in very contrasted velocity models: a massively parallel approach and its associated tools. *Geophysical Journal International* **105** (1), 271–284.

Schnaebele R. 1948. *Monographie géologique du champ pétrolifère de Pechelbronn*. Mémoire du Service de la Carte Géologique d'Alsace et de Lorraine.

Tarantola A. (ed.). 2005. *Inverse problem theory and methods for model parameter estimation.* Society for Industrial and Applied Mathematics.

Tarantola A. and Valette B. 1982. Inverse problems = quest for information. *Journal of Geophysics* **50**, 159–170.

Tukey J.W. 1977. *Exploratory Data Analysis.* Addison-Wesley. ISBN 0201076160.

Wentzel F. and Brun J.-P. 1991. A deep Reflection Seismic Line across theNorthern Rhine Graben. *Earth and Planetary Science Letters* **104**, 140–150.

Wittlinger G., Herquel G. and Nakache T. 1993. Earthquake location in strongly heterogeneous media. *Geophysical Journal International* **115** (3), 759–777.

Acknowledgment

This work was conducted in the framework of the excellence laboratory "Labex G-EAU-THERMIE PROFONDE" (University of Strasbourg). It was funded by the French National Research Agency, as part of the French "Investments for the future" program, by the Energie Baden-Württemberg AG (EnBW), the French institution CNRS, and by the French-German University (DFH-UFA). We wish to thank the ECOGI joint venture and the Électricité de Strasbourg – Géothermie company (ESG) for sharing data. We are grateful to N. Cuenot (EEIG "Heat Mining") for sharing his experience on the Soultz raw seismic data and to A. Genter for fruitful discussions on the Soultz experiments. We also thank L. and C. Dorbath for providing the seismic data catalogues and sharing their knowledge on the datasets.